Journal of Applied Fluid Mechanics, Vol. 7, No. 1, pp. 135-145, 2014.
Available online at www.jafmonline.net, ISSN 1735-3572, EISSN 1735-3645.
DOI: 10.36884/jafm.7.01.19426

An HAM Analysis of Stagnation-Point Flow of a Nanofluid over a Porous Stretching Sheet with Heat Generation

A. Malvandi[1†], F. Hedayati[2] and M. R. H. Nobari[1]

[1] *Mechanical Engineering Department, Amirkabir University of Technology, Tehran, Iran*
[2] *Department of Mechanical Engineering, Islamic Azad University, Sari Branch, Sari, Iran*

†Corresponding Author Email: *amirmalvandi@aut.ac.ir*

(Received February 8, 2013; accepted April 3, 2013)

ABSTRACT

Steady two-dimensional stagnation point flow and heat transfer of a nanofluid over a porous stretching sheet is investigated analytically using the Homotopy Analysis Method (HAM). The employed model for nanofluid includes two-component four-equation non-homogeneous equilibrium model that incorporates the effects of Brownian diffusion and thermophoresis simultaneously. The basic partial boundary layer equations have been reduced to a two-point boundary value problem via similarity variables. The effects of thermophoresis number (Nt), Brownian motion number (Nb), suction/injection parameter (S), source/sink parameter (λ), permeability parameter (k_1), stretching parameter (a/b) and Lewis number (Le) on the temperature and nanoparticle concentration profiles are studied in detail. Moreover, special attention is paid on the variations of reduced Nusselt and Sherwood number on the effects of physical parameters. The obtained results indicate that for $N_b > 2$, reduced Sherwood number remains constant; however, $N_b < 0.5$ corresponds to negative Sherwood number, i.e. concentration rate is reversed.

Keywords: Stagnation-point, Stretching sheet, Homotopy analysis method, Nanofluid, Brownian motion.

NOMENCLATURE

a,b,c	constants	Q_0	dimensional heat generation/absorption (kg.m^2/s)
C	nanoparticle volume fraction	Re	Reynolds number
D_B	Brownian diffusion coefficient	Sh	Sherwood number
D_T	thermophoresis diffusion coefficient	T	temperature (1/K)
k	permeability of the porous medium (m^2)	α_m	thermal diffusivity (m^2/s)
k_1	permeability parameter	τ	parameter defined by $(\rho c)_P / (\rho c)_f$
Le	Lewis number	η	similarity variable
Nb	Brownian motion parameter	μ	dynamic viscosity (kg/m·s)
Nt	thermophoresis parameter	λ	heat source/sink
Nu	Nusselt number	ϕ	rescaled nanoparticle volume fraction
n	stretching parameter	w	condition on the sheet
Pr	Prandtl number	∞	ambient conditions

1. ELECTRONIC SUBMISSION

Stagnation point flow has been attracted considerable attention by many authors through the years. Hiemenz (1911) developed an exact solution of the two dimensional stagnation point flow by using the similarity solution. Then, Homann (1936) extended the problem to the axisymmetric three dimensional stagnation point flow. Later on, different concepts and applications of stagnation point have been investigated in many fluid flow and heat transfer problems (Layek *et al.* 2007; Paullet and Weidman 2007; Wang 2008; Bachok *et al.* 2010; Bhattacharyya 2011; Hamad and Pop 2011; Rosali *et al.* 2011; Chamkha and Ahmed 2011; Gangadhar 2012; Singh *et al.* 2012; Veerraju *et al.* 2012 and Mahapatra and Nandy 2013).

Based on recent studies, scientists have realized that a more effective way to cool different parts of industrial setups is needed which has been responded by using nanofluids in which nanometer-sized particles are added into the working fluid. These tiny particles have high thermal conductivity, so the mixed fluids have better thermal properties. The materials of these nanoscale particles are aluminum oxide (Al2O3), copper (Cu), copper oxide (CuO), gold (Au), etc., that are suspended in base fluids such as water, oil, acetone and ethylene glycol. The main obstacle in this field is how to keep the particles suspended in the static fluid homogeneously. It is noteworthy to say that nanofluids' behavior are modeled mathematically and experimentally by many researchers which can be found in Mustafa *et al.* (2011), Alsaedi *et al.* (2012) and Bachok *et al.* (2012).

To obtain accurate solution of above-mentioned problems, numerical techniques have been developed for years but due to some restrictions (Xu et al. (2008)), analytical approaches have been considered as alternative techniques. Perturbation techniques are the most common methods which are widely applied in science and engineering (Prober and Stewart 1963; Aziz and Benzies 1976; Skobelev and Struminskii 1977). Lack of perturbation techniques are that they strongly depend upon small/large physical parameters, so they cannot apply to strongly nonlinear problems. Hence, non-perturbation techniques such as Homotopy Perturbation method (Malvandi *et al.* 2012) and Variational Iteration Method (Hedayati *et al.* 2012) appeared in order to omit the dependency to small/large parameters. It must be noted that, these methods cannot ensure the convergence of series solution. On the other hand, The Homotopy Analysis Method (HAM) proposed by Liao (2012), is a general analytical approach to obtain series solutions of strongly nonlinear equations which can provides us a simple way to ensure the convergence of solutions series. In addition, we have great freedom to choose a proper base function to approximate a nonlinear problem. Therefore, the HAM is valid even for strongly nonlinear problems. Moreover, in contrast with numerical methods, it can be implemented with boundary condition at infinity; problems such as boundary layers have boundary condition at infinity and numerical methods are not able to evaluated infinity without the aid of previous studies, see Liao (2012).

To the best of author's knowledge, no analytical studies have thus far been reported with regard to the boundary layer stagnation-point flow on a heated porous stretching sheet saturated with a nanofluid. Recently, Hamad and Ferdows (2012) studied the problem numerically with similarity solution. It is not surprising that their numerical results are limited to only special parameters that consistent with presumed similarity variable at infinity. However, the presented analytical results are independent to the value of similarity variable at infinity and cover a wide range of physical parameter. This method has been used by many authors in the wide range of engineering problems (Ziabakhsh *et al.* 2009, Hassani *et al.* 2011, Si *et al.* 2011). Moreover, the effects of non-dimensional parameters such as Prandtl number Pr, Lewis number Le, Brownian motion number N_b and thermophoresis number N_t on the Nusselt and Sherwood numbers are investigated.

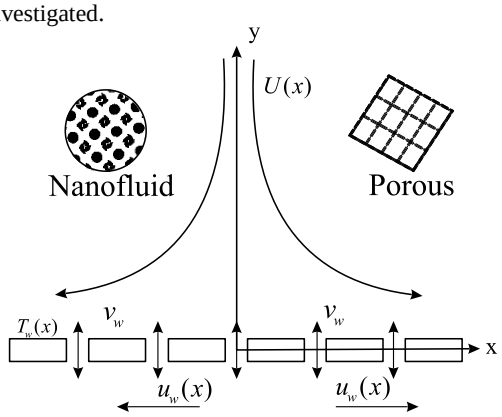

Fig. 1. Geometry of physical domain.

2. GOVERNING EQUATION

Consider the steady laminar two-dimensional flow near a stagnation-point at a porous surface saturated by a nanofluid as shown in Fig. 1. It is assumed that temperature and concentration at the surface have constant values of T_w and C_w respectively, while the ambient temperature and concentration beyond boundary layer has constant values T_∞ and C_∞ respectively. The coordinates x, y are taken with the origin O at the stagnation point. Two opposite forces are applied along the x-axis similarly so that the wall is stretched while the position of the origin is kept fixed. The boundary layer equations governing the flow and heat transfer in the presence of heat source/sink can be expressed as

$$\frac{\partial u}{\partial x}+\frac{\partial v}{\partial y}=0 \tag{1}$$

$$u\frac{\partial u}{\partial x}+v\frac{\partial u}{\partial y}=U(x)\frac{\partial U(x)}{\partial x}+\nu\frac{\partial^2 u}{\partial y^2}+\frac{\nu}{k}(U(x)-u) \tag{2}$$

$$u\frac{\partial T}{\partial x}+v\frac{\partial T}{\partial y}=\alpha\frac{\partial^2 T}{\partial y^2}+\frac{Q_0}{\rho C_p}(T-T_\infty)+\tau\left[D_B\frac{\partial C}{\partial y}\frac{\partial T}{\partial y}+\frac{D_T}{T_\infty}\left(\frac{\partial T}{\partial y}\right)^2\right] \tag{3}$$

$$u\frac{\partial C}{\partial x}+v\frac{\partial C}{\partial y}=D_B\frac{\partial^2 C}{\partial y^2}+\frac{D_T}{T_\infty}\left(\frac{\partial^2 T}{\partial y^2}\right) \tag{4}$$

Subject to the boundary conditions

$$\begin{cases} u=u_w(x)=bx,\ v=v_w,\ T=T_w, \\ C=C_w \end{cases} \quad \text{At } y=0$$
$$\begin{cases} u\to U(x)=ax,\ T\to T_\infty, \\ C\to C_\infty \end{cases} \quad \text{As } y\to\infty \tag{5}$$

where u and v are the velocity components along the x and y coordinates, $U(x)$ the stagnation point velocity of the free stream, ρ_f is the density of the

base fluid, α_m is the thermal diffusivity, ν is the kinematic viscosity, a,b the positive constant, D_B the Brownian diffusion coefficient, D_T is the thermophoretic diffusion coefficient, τ is the ratio between the effective heat capacity of the nanoparticle material and heat capacity of the fluid, C and T are the volumetric volume expansion coefficient and local temperature respectively, ρ_p the density of the particles, k is the permeability of the porous medium and finally Q_0 is the dimensional heat generation or absorption coefficient. With introduction of the following similarity parameters

$$\varphi = xf(\eta), \quad \eta = \frac{c}{\nu}y, \qquad \theta(\eta) = \frac{T - T_\infty}{T_w - T_\infty}, \quad \phi(\eta) = \frac{C - C_\infty}{C_w - C_\infty} \tag{6}$$

Equations (1)-(4) collapse into

$$f''' + ff'' - f'^2 + \frac{a^2}{b^2} + k_1\left(\frac{a}{b} - f'\right) = 0 \tag{7}$$

$$\frac{1}{Pr}\theta'' + f\theta' + \lambda\theta + Nb\theta'\phi' + Nt\theta'^2 = 0 \tag{8}$$

$$\phi'' + Lef\phi' + \frac{Nt}{Nb}\theta'' = 0 \tag{9}$$

with the transformed boundary condition Eq. (5)

$$\text{At} \quad \eta = 0: \quad f = S, \; f' = 1, \; \theta = 1, \; \phi = 1$$
$$\text{As} \quad \eta \to \infty: \quad f' \to \frac{a}{b}, \; \theta \to 0, \; \phi \to 0 \tag{10}$$

where $'$ denotes differentiation with respect to η and the out coming non-dimensional parameters are

$$Nb = \frac{(\rho c)_p D_B (C_w - C_\infty)}{(\rho c)_f \nu}, \quad Pr = \frac{\nu}{\alpha}$$
$$Nt = \frac{(\rho c)_p D_T (T_w - T_\infty)}{(\rho c)_f \nu T_\infty}, \quad Le = \frac{\nu}{D_B} \tag{11}$$

where Pr, Le, Nb, Nt denote the Prandtl number, the Lewis number, the Brownian motion parameter and the thermophoresis parameter respectively. According to Bachok *et al.* (2012), the local Nusselt and Sherwood numbers can be defined as:

$$Nu = \frac{xq_w}{K(T_w - T_\infty)}, \quad Sh = \frac{xq_m}{D_B(C_w - C_\infty)}, \quad C_f = \frac{\tau_w}{\rho u_\infty^2} \tag{12}$$

Here τ_w is the surface shear stress and q_w, q_m are heat and mass flux at the surface respectively, and are defined as follows

$$\tau_w = \mu\left(\frac{\partial u}{\partial y}\right)\Big|_{y=0} \tag{13}$$

$$q_w = -K(T_w - T_\infty)x^{\frac{-1}{2}}\sqrt[2]{\frac{a}{2\nu}}\theta'(0) \tag{14}$$

$$q_m = -D_B(C_w - C_\infty)x^{\frac{-1}{2}}\sqrt[2]{\frac{a}{2\nu}}\phi'(0) \tag{15}$$

It is worth mentioning that using dimensionless variables Eq. (6), the rate of heat and mass transfer and skin friction can be written as

$$\frac{Nu}{\sqrt[2]{Re_x}} = -\theta'(0), \quad \frac{Sh}{\sqrt[2]{Re_x}} = -\phi'(0), \quad \sqrt[2]{2Re_x}C_f = f''(0). \tag{16}$$

Like Bachok *et al.* (2012), in the present context $Nu/\sqrt{Re_x}$, $Sh/\sqrt{Re_x}$ and $\sqrt{2Re_x}C_f$ are referred as the reduced Nusselt number, reduced Sherwood number and reduced skin friction coefficient which are represented by $-\theta'(0)$, $-\phi'(0)$ and $f''(0)$ respectively.

3. SEMI ANALYTICAL SOLUTION

For HAM solutions, the appropriate initial guesses can be chosen as:

$$f_0(\eta) = \frac{a}{b}x + (1 - \frac{a}{b})(1 - e^{-x}) + S$$
$$\theta_0(\eta) = e^{-\eta}, \phi_0(\eta) = e^{-\eta} \tag{17}$$

and auxiliary linear operators

$$L(f) = f''' - f', \quad L\left(C_1 + C_2e^{\eta} + C_3e^{-\eta}\right)$$
$$L(\theta) = \theta'' - \theta, \quad L\left(C_4e^{\eta} + C_5e^{-\eta}\right) \tag{18}$$
$$L(\phi) = \phi'' - \phi, \quad L\left(C_6e^{\eta} + C_7e^{-\eta}\right)$$

Where c_i $(i = 1-7)$ are constants and $p \in [0,1]$ denotes the embedding parameter and h indicate the non-zero auxiliary parameters. So, the zero-order deformation problems are constructed as follows

$$(1-P)L_1\left[f(\eta;p) - f_0(\eta)\right] = ph_1N_1\left[f,\phi,\theta\right]$$
$$(1-P)L_2\left[\theta(\eta;p) - \theta_0(\eta)\right] = ph_2N_2\left[f,\phi,\theta\right] \tag{19}$$
$$(1-P)L_3\left[\phi(\eta;p) - \phi_0(\eta)\right] = ph_3N_3\left[f,\phi,\theta\right]$$

subject to the following boundary conditions

$$f(0,p) = S \quad f'(0,p) = 1 \quad f'(\infty,p) = \frac{a}{b}$$
$$\theta(0,p) = 1 \quad \theta(\infty,p) = 0 \tag{20}$$
$$\phi(0,p) = 1 \quad \phi(\infty,p) = 0$$

where

$$N_1\left[f,\phi,\theta\right] = \frac{\partial^3 f(\eta,p)}{\partial\eta^3} + f(\eta,p)\frac{\partial^2 f(\eta,p)}{\partial\eta^2} - \left(\frac{\partial f(\eta,p)}{\partial\eta}\right)^2 + \frac{a^2}{b^2} + K_1\left(\frac{a}{b} - \frac{\partial f(\eta,p)}{\partial\eta}\right)$$

$$N_2[f,\phi,\theta]=\frac{1}{Pr}\frac{\partial^2\theta(\eta,p)}{\partial\eta^2}+f(\eta,p)\frac{\partial\theta(\eta,p)}{\partial\eta}$$
$$+\lambda\theta(\eta,p)+Nb\frac{\partial\phi(\eta,p)}{\partial\eta}\frac{\partial\theta(\eta,p)}{\partial\eta}+Nt\left(\frac{\partial\theta(\eta,p)}{\partial\eta}\right)^2$$
$$N_3[f,\phi,\theta]=\frac{\partial^2\phi(\eta,p)}{\partial\eta^2}+Le\left(\frac{\partial\phi(\eta,p)}{\partial\eta}\right)f(\eta,p)$$
$$+\frac{Nt}{Nb}\left(\frac{\partial^2\theta(\eta,p)}{\partial\eta^2}\right) \tag{21}$$

According to the Taylor series with respect to p, the mth-order deformation equations may be achieved

$$L_1[f_m(\tau)-\chi_m f_{m-1}(\tau)]=h_1R_m^f(\eta)$$
$$L_2[\theta_m(\tau)-\chi_m\theta_{m-1}(\tau)]=h_2R_m^\theta(\eta) \tag{22}$$
$$L_3[\phi_m(\tau)-\chi_m\phi_{m-1}(\tau)]=h_3R_m^\phi(\eta)$$

with

$$f_m(\eta)=\frac{1}{m!}\frac{\partial^m f(\eta,p)}{\partial p^m},\ \theta_m(\eta)=\frac{1}{m!}\frac{\partial^m\theta(\eta,p)}{\partial p^m},$$
$$\phi_m(\eta)=\frac{1}{m!}\frac{\partial^m\phi(\eta,p)}{\partial p^m} \tag{23}$$

and the boundary conditions are

$$f_m(0)=f'_m(0)=f'_m(\infty)=0$$
$$\theta_m(0)=\theta_m(\infty)=0 \tag{24}$$
$$\phi_m(0)=\phi_m(\infty)=0$$

where

$$R_m^f=f'''_{m-1}+\sum_{n=0}^{m-1}f_{m-1-n}f''_n-\sum_{n=0}^{m-1}f'_{m-1-n}f'_n$$
$$+(1-\chi_m)\left(\frac{a^2}{b^2}+k_1\frac{a}{b}\right)-k_1\sum_{n=0}^{m-1}f'$$
$$R_m^\theta=\frac{1}{Pr}\theta''_{m-1}+\sum_{n=0}^{m-1}f_{m-1-n}\theta'_n+\lambda\theta \tag{25}$$
$$+N_b\sum_{n=0}^{m-1}\phi'_{m-1-n}\theta'_n+N_t\sum_{n=0}^{m-1}\theta'_{m-1-n}\theta'_n$$
$$R_m^\phi=\phi''_{m-1}+Le\sum_{n=0}^{m-1}f_{m-1-n}\phi'_n+\frac{N_t}{N_b}\theta''_{m-1}$$

and

$$\chi_m=\begin{cases}0 & m\le 1\\ 1 & m>1\end{cases} \tag{26}$$

which $\hbar_i\,(i=1,2,3)$ is chosen in such a way that these three series are convergent at $p=1$. Equation (22) represents the system of non-homogeneous linear differential equations whose general solutions are the sum of complementary and particular solutions which can be expressed as:

$$f_m(\eta)=f_m^*(\eta)+C_1^m+C_2^m\,e^{\eta}+C_3^m\,e^{-\eta}$$
$$\theta_m(\eta)=\theta_m^*(\eta)+C_4^m\,e^{\eta}+C_5^m e^{-\eta} \tag{27}$$
$$\phi_m(\eta)=\phi_m^*(\eta)+C_6^m\,e^{\eta}+C_7^m\,e^{-\eta}$$

To determine the values of these unknown constants, the boundary conditions Eq. (24) may be applied. Invoking the boundary conditions for f_m,θ_m,ϕ_m as $\eta\to\infty$, it can be obtained

$$C_2^m=C_4^m=C_6^m=0 \tag{28}$$

Similarly using the conditions at $\eta=0$ in Eq. (27), it can be deduced

$$C_1^m=-C_3^m-f_m^*(0),\ C_3^m=\left.\frac{\partial f_m^*(\eta)}{\partial\eta}\right|\eta=0$$
$$C_5^m=-\theta_m^*(0),\quad C_7^m=-\phi_m^*(0) \tag{29}$$

Hence, the velocity $f(\eta)$, the tempreture $\theta(\eta)$ and the concentration $\phi(\eta)$ can be obtained by

$$f(\eta)=f_0(\eta)+\sum_{m=1}^{\infty}f_m(\eta)$$
$$\theta(\eta)=\theta_0(\eta)+\sum_{m=1}^{\infty}\theta_m(\eta) \tag{30}$$
$$\phi(\eta)=\phi_0(\eta)+\sum_{m=1}^{\infty}\phi_m(\eta)$$

4. RESULTS AND DISCUSSION

The system of Eqs. (7)-(9) and the boundary condition of Eq. (10) have been solved analytically via Homotopy Analysis Method (HAM). As pointed by Liao (2012), the convergence rate of approximation for the HAM solution strongly depend on the value of auxiliary parameter, $\hbar_i\,(i=1,2,3)$. In order to seek the permissible values of $\hbar_1,\hbar_2$ and $\hbar_3$ of the functions of $f'''(0)$, $\theta'(0)$ and $\phi'(0)$ curves are plotted at 20th-order of approximations. Figures. 2(a) and 2(b) clearly depict the acceptable range, for values of $-0.7<\hbar_1<-0.2$ and $-0.6<\hbar_2,\hbar_3<-0.2$ respectively. The present calculations are carried out based on the value of $\hbar_1=-0.6$ and $\hbar_2=-0.3$. Furthermore, the best accuracy of the results is compared with the previous literatures in Table 1.

Table1 Comparison of results for $-\theta'(0)$ when $\lambda = Nb = Nt = S = a/b = k_1 = 0$.

Pr	Present results	Hamad And Ferdows (2012)	Wang (2008)
0.07	0.06557	0.06556	0.0656
0.2	0.16911	0.16909	0.1691
0.7	0.45391	0.45391	0.4539
2	0.91138	0.91136	0.9114

Before goes farther in the results, it is worth to describe the physical aspects of governing parameters more which appears in the nanofluid's model, i.e. Brownian motion and thermophoresis. Brownian motion (Nb) can be observed as random drifting of suspended nanoparticles, on the other hand, thermophoresis (Nt) is nanoparticles migration due to imposed temperature gradient across the fluid. A mentioned phenomenon is the two important slip mechanisms which emerge as a result of nanoparticles' slip velocity to the base fluid. For hot surfaces, due to repelling the sub-micron sized particles, the thermophoresis tends to blow nanoparticle volume fraction boundary layer away from the surface. Also, owing to size scale of particles, Brownian motion has significant influence on the surrounding liquids. Temperature and concentration profiles are analyzed in Figs. 3-5. In Figs. 3(a) and 3(b) the variation of temperature and concentration versus η at three different Lewis numbers are depicted. It is evident from the figures that dimensionless temperature is almost independent of Le but the concentration profile decreases when Le increases. Moreover, it can be realized that for Le<1, the concentration trend on the wall reverses; this leads to a noticeable rise in the concentration boundary layer.

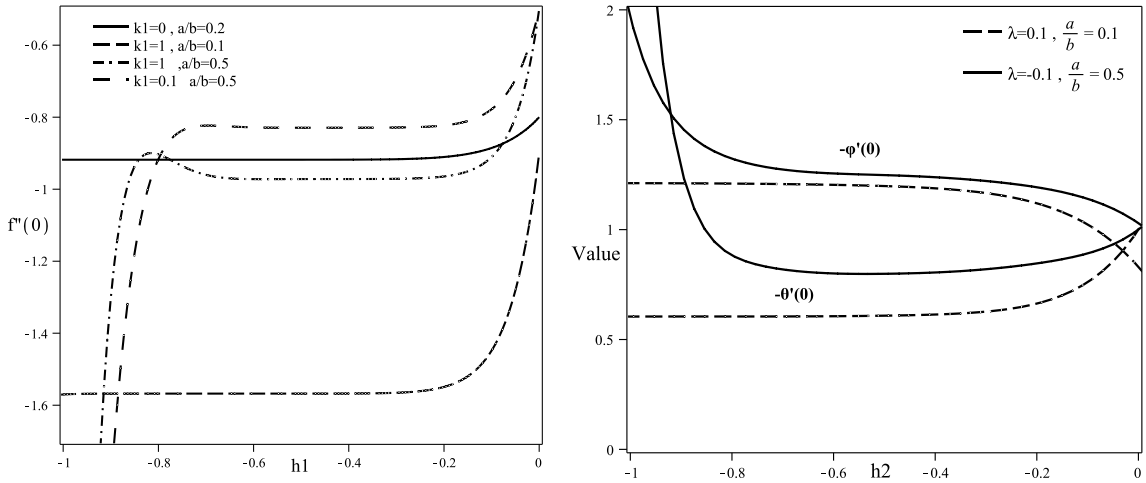

(a) *(b)*

Fig. 2. $f''(0)$ plots for determining the optimum h_1 coefficient. (b) $\theta'(0)$ plots for determining the optimum h_2 and h_3 coefficients

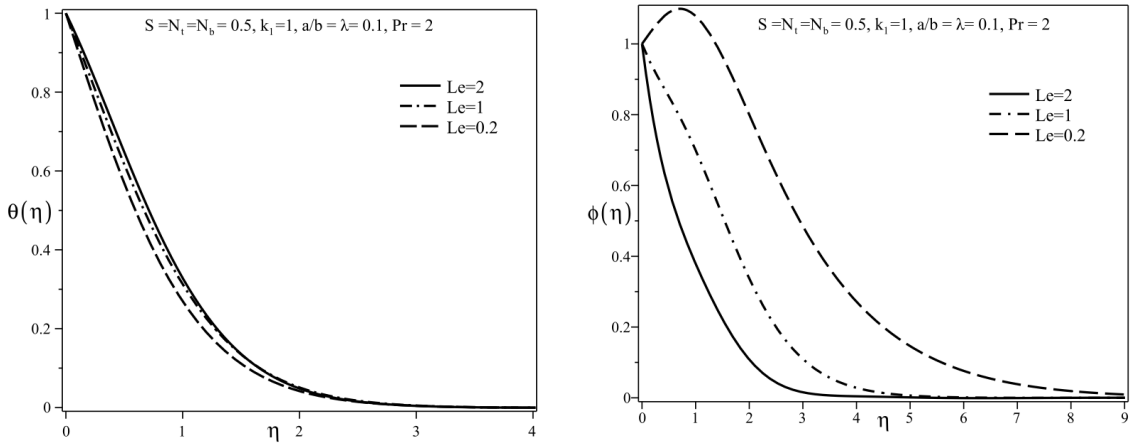

(a) *(b)*

Fig. 3. Effects of Lewis number on (a) Temperature, (b) Concentration

Next, we focused on the thermophoresis parameter effects on the temperature and concentration profiles which are displayed in Figs. 4(a) and 4(b) respectively. As is obvious, an increase in the thermophoresis parameter, Nt , increase both of fluid temperature and nanoparticle concentration. It must be mentioned that for $Nt > 2$, the parameter affects the temperature profile significantly which distinguishes this profile from conventional fluid. The effects of Nb on the temperature and concentration profiles are revealed in Figs. 5(a) and 5(b) respectively. It is obvious that as Nb increases, the values of θ increases as well. Unlike θ , the values of ϕ , decreases by increasing the Nb. Concerning Fig. 5(b), it can be realized that for the values of $Nb < 0.5$, the variational trend at the wall changes. It is noteworthy to say that Brownian motion can be observed as random drifting of suspended nanoparticles, on the other hand, thermophoresis is nanoparticle migration due to imposed temperature gradient across the fluid. Mentioned mechanisms are two important slip mechanisms which appears as a result of nanoparticles' slip velocity to the base fluid.

Effect of Lewis number on the reduced Nu and Sh numbers inside the boundary layer are plotted in Figs. 6(a) and 6(b) respectively. It is clear that an increase in the Lewis number leads to a decrease in the Nusselt number; however, Sherwood number increases with increasing in Le . It is worth mentioning that at lower values of Lewis numbers, Sherwood number is negative i.e. reverse mass transfer occurs. In addition, for heat source $\lambda > 0$, reduced Nusselt number decreases but reduced Sherwood number climbs up. It is true to say that λ has negligible effects on trends of Nu and Sh versus Le . In Figs. 7(a) and 7(b) Reduced Nusselt and Sherwood variations versus Prandtl number have been plotted. Accordingly, it can be realized that when Pr increases, unlike Nusselt number, the values of Sherwood number decreases.

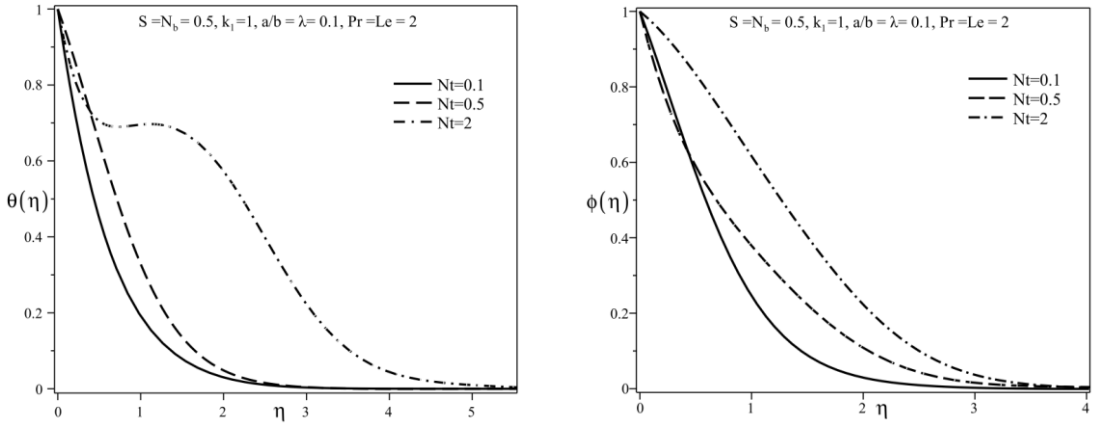

(a) *(b)*

Fig. 4. Effects of thermophoresis parameter on (a) Temperature, (b) Concentration

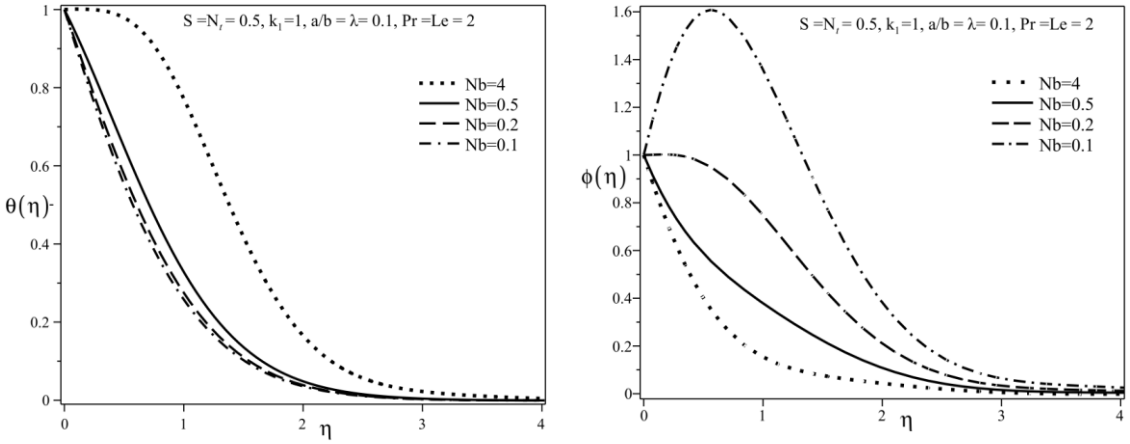

(a) *(b)*

Fig. 5. Effects of Brownian motion parameter on (a) Temperature, (b) Concentration

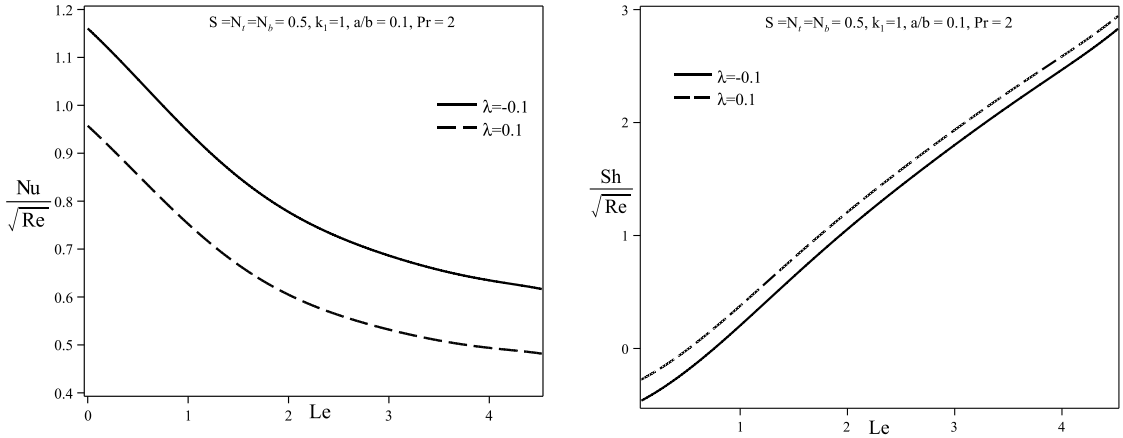

Fig. 6. Effects of Lewis number on (a) Reduced Nusselt number, (b) Reduced Sherwood number

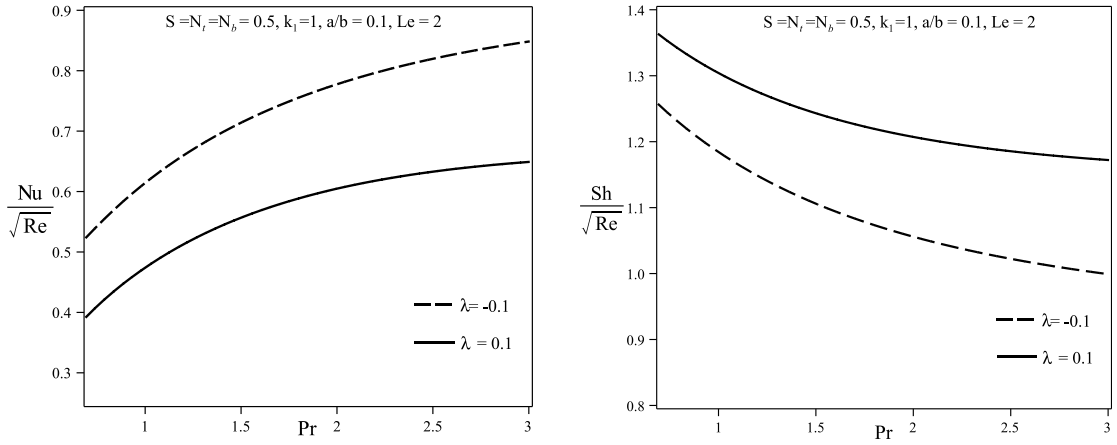

Fig. 7. Effects of Prandtl number on (a) Reduced Nusselt number, (b) Reduced Sherwood number

Figures 8(a) and 8(b) show the variation of reduced Nusselt and Sherwood numbers versus thermophoresis parameter. It is obvious that when Nt increases, the values of reduced Sherwood and Nusselt numbers decrease. Indeed, it can be seen that for $Nt > 2$, thermophoresis parameter has minor effects on reduced Sherwood number.

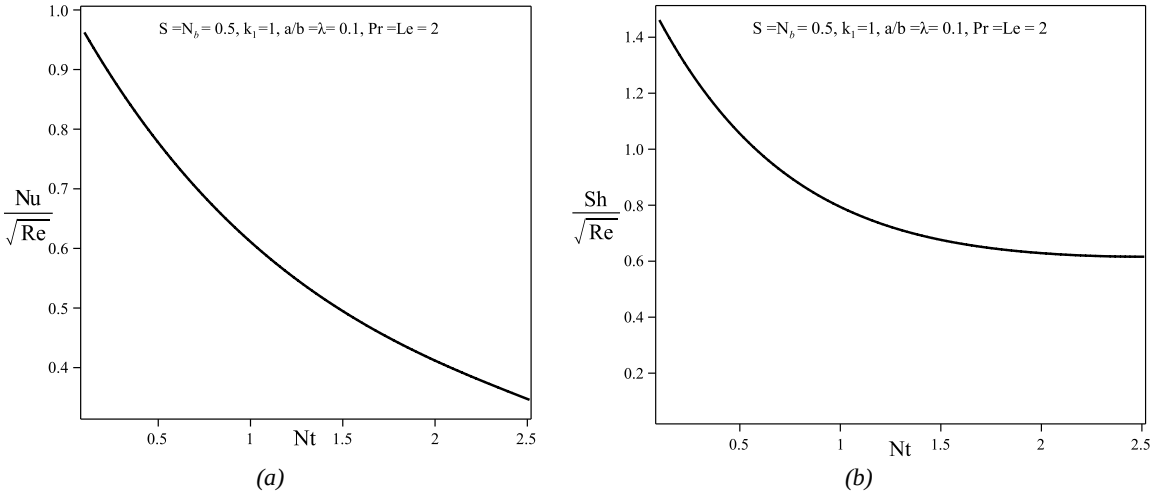

Fig. 8. Effects of thermophoresis parameter on (a) Reduced Nusselt number, (b) Reduced Sherwood number

The effect of Brownian motion Nb on the reduced Nu and Sh numbers inside the boundary layer are plotted in Figs. 9(a) and 9(b) respectively. As is evident, an increase in Nb , unlike the Nu profile, is accompanied by an increase of Sh number. Considering Fig. 9(b), there is a special value for $Nb \approx 2$ beyond which the values of Sh number is independent of Nb . Also it can be seen that for small value of Nb , opposite transfer, i.e. negative Sherwood number, occurs.

Figures 10(a) and 10(b) display the effects of source/sink parameter λ on Nu and Sh respectively. As λ increases, unlike Sh , Nu decreases. It is worth mentioning that the effects of λ on Nu , depends on a/b . Moreover, as can be seen in Fig. 10b, the ratio of a/b has greater impacts on Sh for $\lambda < 0$. Finally The effects of permeability, k_1 on Nu and Sh have been investigated in Figs. 11(a) and 11(b) respectively. Both figures indicate a declining trend when k_1 increases. It is obvious that k_1 has stronger effects on the profiles when the velocity ratio becomes very small.

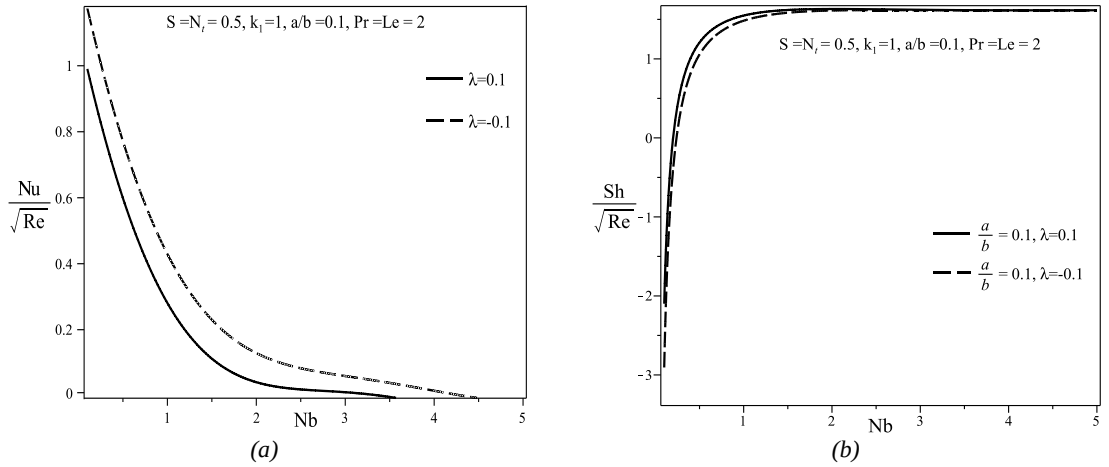

Fig. 9. Effects of Brownian motion parameter on (a) Reduced Nusselt number, (b) Reduced Sherwood number

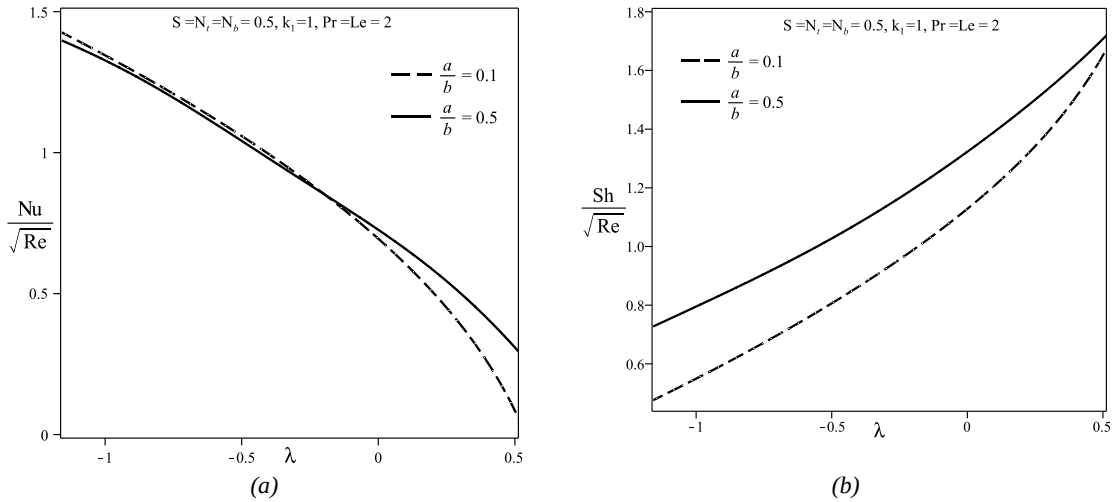

Fig. 10. Effects of heat source/sink on (a) Reduced Nusselt number, (b) Reduced Sherwood number

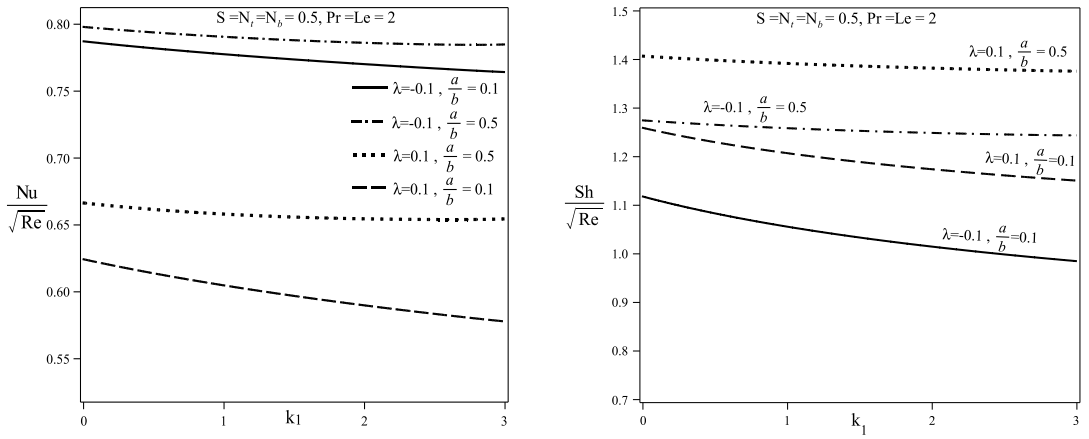

(a) *(b)*

Fig. 11. Effects of permeability on (a) Reduced Nusselt number, (b) Reduced Sherwood number

5. CONCLUSION

In this paper, the two-dimensional stagnation-point flow and heat transfer towards a heated porous stretching sheet saturated with a nanofluid with heat source and suction / blowing boundary condition are studied. The transformed ODE equations for mass, momentum, energy and nanoparticles conservation have been solved analytically with the homotopy analysis method (HAM). The effects of various non-dimensional parameters on the temperature and concentration profiles are studied in details. Results for the reduced Nusselt number (wall heat transfer rate) and reduced Sherwood number (wall mass transfer rate) are presented. The main results of the paper can be summarized as follows:

- It is found that when the Brownian motion parameter Nb increases, unlike temperature θ, the concentration ϕ decreases. However, an increase in the thermophoresis parameter, Nt, leads to an increase in the values of temperature θ and concentration ϕ both.

- Rising in Brownian motion parameter Nb, corresponds with climbing in reduced Sherwood number up and falling in reduced Nusselt number. Also, increasing the thermophoresis parameter Nt, increases reduced Nusselt number and decreases reduced Sherwood number.

- Both of reduced Nusselt and Sherwood numbers decrease as permeability parameter k_1 grows.

- The influence of heat source/sink λ is to decrease reduced Nusselt number and to increase reduced Sherwood number.

- With increasing in Prandtl number $\Pr$, unlike the Nusselt number, the values of Sherwood number decreases.

- Reduced Nusselt number declines with increasing in Lewis number; on the other hand, reduced Sherwood number increases.

REFERENCES

Alsaedi, A., M. Awais and T. Hayat (2012), Effects of heat generation/absorption on stagnation point flow of nano fluid over a surface with convective boundary conditions. *Communications in Nonlinear Science and Numerical Simulation*.

Aziz, A. and J. Y. Benzies (1976). Application of perturbation techniques to heat-transfer problems with variable thermal properties. *International Journal of Heat and Mass Transfer*, 19, 3- 5.

Bachok, N., A. Ishak and I. Pop (2010). Mixed convection boundary layer flow near the stagnation point on a vertical surface embedded in a porous medium with anisotropy effect. *Transport in Porous Media*, 82, 10.

Bachok, N., A. Ishak and I. Pop (2012). Boundary layer flow over a moving surface in a nano fluid with suction or injection. *Acta Mechanica Sinica*, 28, 6.

Bhattacharyya, K. (2011). Dual solutions in boundary layer stagnation-point flow and mass transfer with chemical reaction past a stretching/shrinking sheet. International *Communications in Heat and Mass Transfer*. 38(7), 5.

Chamkha, A. J. and S. E. Ahmed (2011). Similarity Solution for Unsteady MHD Flow Near a Stagnation Point of a Three-Dimensional Porous Body with Heat and Mass Transfer, Heat Generation/Absorption and Chemical Reaction. *Journal of Applied Fluid Mechanics*, 4(3), 87-94.

Gangadhar, K. (2012). Soret and Dufour Effects on Hydro Magnetic Heat and Mass Transfer over a

Vertical Plate with a Convective Surface Boundary Condition and Chemical Reaction. *Journal of Applied Fluid Mechanics,* 6(1), 95-105.

Hamad, M. and I. Pop (2011). Scaling transformations for boundary layer flow near the stagnation-point on a heated permeable stretching surface in a porous medium saturated with a nano fluid and heat generation/absorption effects. *Transport in Porous Media,* 87, 9.

Hamad, M. A. A. and M. Ferdows (2012). Similarity solution of boundary layer stagnation-point flow towards a heated porous stretching sheet saturated with a nano fluid with heat absorption/generation and suction/blowing: A lie group analysis. *Communications in Nonlinear Science and Numerical Simulation*, 17(18), 132

Hassani, M., M. M. Tabar, H. Nemati, G. Domairry and F. Noori (2011). An analytical solution for boundary layer flow of a nano fluid past a stretching sheet. *International Journal of Thermal Sciences*, 50(11), 7.

Hedayati, F., D. D. Ganji, S. M. Hamidi and A. Malvandi (2012). An Analytical Study on a Model Describing Heat Conduction in Rectangular Radial Fin with Temperature-Dependent Thermal Conductivity, *International Journal of Thermophysics*, 33(6), 1042-1054.

Hiemenz, K. (1911). Die grenzschicht an einem in den gleichformigen ussigkeitsstrom eingetauchten geraden kreiszylinder. *Dingler's Polytechnic Journal*.

Homann, F. (1936). Der einuss grosser zhigkeit bei der strmung um den zylinder und um die kugel. *Zeit angew Math. Mech*.

Layek, G. C., S. Mukhopadhyay and S. A. Samad (2007). Heat and mass transfer analysis for boundary layer stagnation-point flow towards a heated porous stretching sheet with heat absorption/generation and suction/blowing. *International Communications in Heat and Mass Transfer*, 34(3), 9

Liao, S. (2012). *Homotopy Analysis Method in Nonlinear Dierential Equations*. Beijing and Heidelberg, Springer.

Mahapatra, T. R. and S. K. Nandy (2013). Momentum and Heat Transfer in MHD Axisymmetric Stagnation-Point Flow over a Shrinking Sheet. *Journal of Applied Fluid Mechanics,* 6(1), 121-129.

Malvandi, A., D. D. Ganji, F. Hedayati, M. H. Kaffash and M. Jamshidi (2012). Series Solution of Entropy Generation Toward an Isothermal Flat Plate. *Thermal Science*, 16(5), 1289-1295.

Mustafa, M., T. Hayat, I. Pop, S. Asghar and S. Obaidat (2011). Stagnation-point flow of a nano fluid towards a stretching sheet. *International Journal of Heat and Mass Transfer*, 54(6).

Paullet, J. and P. Weidman (2007). Analysis of stagnation point flow toward a stretching sheet. *International Journal of Non-Linear Mechanics*, 49(9), 7.

Prober, R. and W. E. Stewart (1963). Transport phenomena in wedge flows: Perturbation solutions for small mass transfer rates. *International Journal of Heat and Mass Transfer*, 6(3), 8.

Rosali, H., A. Ishak and I. Pop (2011). Stagnation point flow and heat transfer over a stretching/shrinking sheet in a porous medium. *International Communications in Heat and Mass Transfer*, 38(8), 3.

Si, X., L. Zheng, X. Zhang and Y. Cha (2011). Homotopy analysis solutions for the asymmetric laminar flow in a porous channel with expanding or contracting walls. *Acta Mechanica Sinica*, 27(6).

Singh, P., D. Sinha and N. S. Tomer (2012). Oblique Stagnation-Point Darcy Flow towards a Stretching Sheet. *Journal of Applied Fluid Mechanics,* 5(3), 29-37.

Skobelev, B. I. and V. V. Struminskii (1977). Nonlinear perturbation development in two-dimensional laminar flows. *Journal of Applied Mathematics and Mechanics,* 41(5), 4.

Veerraju, N., K. S. Srinivasa Babu and C. N. B. Rao (2012). Mixed Convection at a Vertical Plate in a Porous Medium with Magnetic Field and Variable Viscosity. *Journal of Applied Fluid Mechanics*, 5(4), 53-62.

Wang, C. Y. (2008). Stagnation flow towards a shrinking sheet. *International Journal of Non-Linear Mechanics*, 43(5), 5

Xu, H., S. Liao and I. Pop (2008). Series solutions of unsteady free convection flow in the stagnation-point region of a three-dimensional body. *International Journal of Thermal Sciences,* 47(8).

Ziabakhsh, Z., G. Domairry and H. Bararnia (2009). Analytical solution of non-newtonian micropolar fluid flow with uniform suction/blowing and heat

generation. *Journal of the Taiwan Institute of Chemical Engineers*, 40(4), 8.